Inorg. Chem. **2003**, *42*, 7789–7798

Multimetallic Ruthenium(II) Complexes as Electrochemiluminescent Labels

Mara Staffilani,[§] Eva Hŏss,[‡] Ulla Giesen,[‡] Erich Schneider,[‡] František Hartl,[§] Hans-Peter Josel,*[,‡] and Luisa De Cola*[,§]

IMC, Molecular Photonic Materials, Universiteit van Amsterdam, Nieuwe Achtergracht 166, 1018 WV Amsterdam, The Netherlands, and Roche Diagnostics GmbH, Nonnenwald 2, 82372 Penzberg, Germany

Received April 23, 2003

Two homometallic complexes containing two and three ruthenium polypyridyl units linked by amino acid lysine (Lys) and the related dipeptide (LysLys) were synthesized and their electrochemical, spectroscopic, and electrochemiluminescence (ECL) properties were investigated. The electrochemical and photophysical data indicate that the two metal complexes largely retain the electronic properties of the reference compound for the separate ruthenium moieties in the two bridged complexes, [4-carboxypropyl-4′-methyl-2,2′-bipyridine]bis(2,2′-bipyridine)-ruthenium(II) complex. The ECL studies, performed in aqueous media in the presence of tri-*n*-propylamine as co-reactant, show that the ECL intensity increases by 30% for the dinuclear and trinuclear complexes compared to the reference. Heterogeneous ECL immunoassay studies, performed on larger dendritic complexes containing up to eight ruthenium units, demonstrate that limitations due to the slow diffusion can easily be overcome by means of nanoparticle technology. In this case, the ECL signal is proportional to the number of ruthenium units. Multimetallic systems with several ruthenium centers may, however, undergo nonspecific bonding to streptavidin-coated particles or to antibodies, thereby increasing the background ECL intensity and lowering the sensitivity of the immunoassay.

Introduction

Since the discovery[1] of the electrogenerated chemiluminescence (ECL) of $[Ru(bpy)_3]^{2+}$ (bpy = 2,2′-bipyridine), this metal complex has played a key role in the development of the ECL and its diverse applications.[2−9]

The ECL of $[Ru(bpy)_3]^{2+}$ can be generated upon charge recombination between the electrogenerated $[Ru(bpy)_3]^{3+}$ and $[Ru(bpy)_3]^{+}$ (ion annihilation mechanism) that leads to population of the emitting triplet metal-to-ligand charge-transfer (^{3}MLCT) excited state.[1,3,4] Alternatively, ECL can be generated upon reaction between $[Ru(bpy)_3]^{3+}$ (or $[Ru(bpy)_3]^{+}$) and a reductant (or oxidant) species.[5,6,10,11]

One of the most important applications for the ECL of $[Ru(bpy)_3]^{2+}$ lies in medical diagnostics, e.g., in immunoassays and DNA-probing assays, where the ruthenium complex, labeling a biological molecule, undergoes an ECL reaction in the presence of tri-*n*-propylamine (TPrA).[5,6,12] The possibility to avoid the well-known radioactive assays, the facile triggering of the electrochemical reaction, the low detection limit (200 fmol dm^{-3}), and the large dynamic range (6 orders of magnitude) are among the most important advantages of the ECL technique over isotope or fluorescence labeling

* To whom correspondence should be addressed. E-mail: ldc@science.uva.nl; hans-peter.josel@roche.com.
§ Universiteit van Amsterdam.
‡ Roche Diagnostics GmbH.

(1) Tokel, N. E.; Bard, A. J. *J. Am. Chem. Soc.* **1972**, *94*, 2862.
(2) Bard, A. J.; Keszthelyi, C. P.; Tachikawa, H.; Tokel, N. E. *Chemilumin. Biolumin. Pap. Int. Conf.* **1973**, 193−208.
(3) Kapturkiewicz, A. *Adv. Electrochem. Sci. Eng.* **1997**, *5*, 1−60.
(4) Bard, A. J.; Faulkner, R. L. *Electrochemical Methods, Fundamentals and Applications*; John Wiley & Sons: New York, 1980.
(5) Lee, W.-Y. *Mikrochim. Acta* **1997**, *127*, 19−39.
(6) Knight, A. W. *Trends Anal. Chem.* **1999**, *18*, 47−62.
(7) Fähnrich, K. A.; Pravda, M.; Guilbault, G. G. *Talanta* **2001**, *54*, 531−559.
(8) Gao, F. G.; Bard, A. J. *Chem. Mater.* **2002**, *14*, 3465−3470.
(9) Buda, M.; Kalyuzhny, G.; Bard, A. J. *J. Am. Chem. Soc.* **2002**, *124*, 6090−6098.
(10) Rubinstein, I.; Bard, A. J. *J. Am. Chem. Soc.* **1981**, *103*, 512−516.
(11) Leland, J. K.; Powell, M. J. *J. Electrochem. Soc.* **1990**, *137*, 3127−3131.
(12) Blackburn, G. F.; Shah, H. P.; Kenten, J. H.; Leland, J.; Kamin, R. A.; Link, J.; Peterman, J.; Powell, M. J.; Shah, A.; Talley, D. B.; Tyagi, S. K.; Wilkins, E.; Wu, T.-G.; Massey, R. J. *Clin. Chem.* **1991**, *37*, 1534−1539.

10.1021/ic034435+ CCC: $25.00 © 2003 American Chemical Society
Published on Web 10/25/2003

techniques.[12−14] Despite the good performance of the ECL assays, higher sensitivity (signal-to-noise ratio) is required because of the increasing demand for accuracy in diagnostics. The enhancement of the ECL efficiency of the label therefore becomes a crucial point.

Several studies have recently dealt with the role of numerous parameters influencing the ECL process of $[Ru(bpy)_3]^{2+}$/TPrA system in aqueous solution, e.g., the electrode surface,[15,16] chemical nature of the co-reactant,[17] and pH dependence.[18] Attempts to increase the ECL efficiency by using complexes with different metal centers have not been very successful.[19−22] Only recently an osmium[18] complex has been reported to exhibit ECL efficiency higher than $[Ru(bpy)_3]^{2+}$ in an aqueous solution. More successful has been the introduction of ruthenium complexes with modified chelating ligands, designed to increase the emission quantum yield. For example, this is the case of the ruthenium tris(4,4′-diphenyl-2,2′-bipyridine) complex[23] that has emission efficiency and ECL signal higher than $[Ru(bpy)_3]^{2+}$.

A promising approach toward the enhancement of the ECL signal of the label is to build up polynuclear systems.[24,25] This strategy has the advantage of providing multiple redox centers, thereby increasing the number of charge recombination events. Fundamental requirements for this improvement are (i) accessibility of the ruthenium centers to the electrode surface and to active TPrA species and (ii) electronic equivalence of the chromophores to avoid intramolecular energy transfer from the excited chromophores to a lowest-lying unoccupied molecular orbital (LUMO) of an acceptor moiety. A possible disadvantage is the exergonic electron transfer between an excited ruthenium unit and a nearby oxidized moiety. A proper choice of the bridging ligand (connector) is then of key importance for a successful design of the multinuclear systems for the ECL reaction. Amino acids and peptides, bearing various functional groups, are versatile molecules to act as bridging ligands connecting the ruthenium bipyridine moieties modified with appropriate substituents.[26−31] Furthermore, their hydrophilic character will enhance the solubility of the multimetallic complexes in water.

We have synthesized dinuclear and trinuclear homometallic complexes containing ruthenium tris(bipyridine) units bound to a bridging ligand by a propoxycarbonyl linker (Chart 1). The employed bridging ligands are the amino acid lysine (Lys)[26,29−32] and the related dipeptide (LysLys), with amino functional groups suitable for the anchoring of the ruthenium units by a peptidic bond and a carboxylic group available for conjugation to a biological molecule. In this work we present the syntheses and the electrochemical, spectroscopic, and ECL investigations of the two complexes, hereafter denoted as **[Ru2−Lys]**$^{4+}$ and **[Ru3−LysLys]**$^{6+}$ (Chart 1). The ECL was performed in a phosphate buffer solution in the presence of TPrA. The influence of nonionic surfactants on the spectroscopy and the ECL of the two complexes are also discussed. The [4-carboxypropyl-4′-methyl-2,2′-bipyridine]bis(2,2′-bipyridine)ruthenium(II) complex,[33,34] **[Ru−Ref]**$^{2+}$ (Chart 1), structurally close to the individual ruthenium moieties in the multimetallic complexes, was investigated as the reference compound.

Furthermore, we report the ECL properties of three large dendritic complexes[35] **[Ru2−Dend]**$^{4+}$, **[Ru4−Dend]**$^{8+}$, and **[Ru8−Dend]**$^{16+}$ containing two, four, and eight ruthenium (tris)bipyridine units, respectively, and bound to a modified progesterone molecule (see Chart 2). The three complexes were also tested in ECL-based progesterone immunoassays, where nanoparticle technology was employed.[12,14]

Experimental Section

Materials. [4-(*N*-succimidyloxycarbonylpropyl)-4′-methyl-2,2′-bipyridine]bis(2,2′-bipyridine)ruthenium(II) dihexafluorophosphate ($[Ru(bpy)_2(bpyOSu)](PF_6)_2$),[12,14,33,34] [4-carboxypropyl-4′-methyl-2,2′-bipyridine]bis(2,2′-bipyridine)ruthenium(II) dihexafluorophosphate[33,34] (**[Ru−Ref]**$(PF_6)_2$)[35] was obtained from Roche Diagnostics GmbH. l-Lysine (Lys, Bachem), N^6-L-lysyl-L-lysine trihydrochloride (Bachem), ammonium hexafluorophosphate (Aldrich), trifluoroacetic acid (TFA, Merck), tri-*n*-propylamine (TPrA, Aldrich), dimethylformamide (Acros, synthesis grade), and acetonitrile (Merck, HPLC grade) were used as received. For electrochemistry, acetonitrile (Acros, synthesis grade) was dried over CaH_2 and freshly distilled under nitrogen prior to use. Tetrabutylammonium hexafluorophosphate (Bu_4NPF_6, Aldrich) was recrystallized twice from ethanol and dried overnight under reduced pressure at 60 °C. Ferrocene (Aldrich) was used as supplied.

Syntheses. [Ru2-Lys](PF$_6$)$_4$. L-(+)-2,6-diamino-*N*-hexanoic acid (Lys, 30 mg, 0.108 mmol) in phosphate buffer solution (10 mL, pH 7.4) was added dropwise to $[Ru(bpy)_2(bpyOSu)](PF_6)_2$ (500 mg, 0.473 mmol) previously dissolved in dimethylformamide (20 mL). After stirring at room temperature overnight, the solvents were

(13) Warner, I. M.; Soper, S. A.; McGown, L. B. *Anal. Chem.* **1996**, *68*, 73R−91R.
(14) Hoyle, N. R.; Eckert, B.; Kraiss, S. *Clin. Chem.* **1996**, *42*, 1576−1578.
(15) Zu, Y.; Bard, A. J. *Anal. Chem.* **2000**, *72*, 3223−3232.
(16) Zu, Y.; Bard, A. J. *Anal. Chem.* **2001**, *73*, 3960−3964.
(17) Knight, A. W.; Greenway, G. M. *Analyst* **1996**, *121*, 101R−106R.
(18) Bruce, D.; Richter, M. M.; Brewer, K. J. *Anal. Chem.* **2002**, *74*, 3157−3159.
(19) Muegge, B. D.; Brooks, S.; Richter, M. M. *Anal. Chem.* **2003**, *75*, 1102−1105.
(20) Lee, S. K.; Bard, A. J. *Anal. Lett.* **1998**, *31*, 2209−2229.
(21) Bolletta, F.; Ciano, M.; Balzani, V.; Serpone, N. *Inorg. Chim. Acta* **1982**, *62*, 207−213.
(22) Bruce, D.; Richter, M. M. *Anal. Chem.* **2002**, *74*, 1340−1342.
(23) McCord, P.; Bard, A. J. *J. Electroanal. Chem.* **1991**, *318*, 91−99.
(24) Richter, M. M.; Bard, A. J.; Kim, W.; Schmehl, R. H. *Anal. Chem.* **1998**, *70*, 310−318.
(25) Zhou, M.; Roovers, J. *Macromolecules* **2001**, *34*, 244−252.
(26) Pan, L. P.; Durham, B.; Wolinska, J.; Millett, F. *Biochemistry* **1988**, *27*, 7180−7184.
(27) Schanze, K. S.; Sauer, K. *J. Am. Chem. Soc.* **1988**, *110*, 1180−1186.
(28) Peek, B. M.; Ross, G. T.; Edwards, S. W.; Meyer, G. J.; Meyer, T. J.; Erickson, B. W. *Int. J. Pept. Protein Res.* **1991**, *38*, 114−123.
(29) Mecklenburg, S. L.; Peek, B. M.; Schoonover, J. R.; McCafferty, D. G.; Wall, C. G.; Erickson, B. W.; Meyer, T. J. *J. Am. Chem. Soc.* **1993**, *115*, 5479−5495.
(30) McCafferty, D. G.; Bishop, B. M.; Wall, C. G.; Hughes, S. G.; Mecklenberg, S. L.; Meyer, T. J.; Erickson, B. W. *Tetrahedron* **1995**, *51*, 1093−1106.
(31) Geisser, B.; Ponce, A.; Alsfasser, R. *Inorg. Chem.* **1999**, *38*, 2030−2037.
(32) Geisser, B.; König, B.; Alsfasser, R. *Eur. J. Inorg. Chem.* **2001**, 1543−1549.
(33) Martin, M. T.; Liang, P.; Dong, L. *Electrochemiluminescent Monitoring of Compounds*; PCT Int. Appl., 1996.
(34) Leland, J. K.; Gudibande, S. R.; Shen, L. *Electrochemiluminescent Labels Having Improved Nonspecific Binding Properties*; PCT Int. Appl., 1997.
(35) Josel, H. P.; Finke, A.; Herrmann, R.; Höss, E.; Marschall, A.; Seidel, C. WO, Patent 9603650A1, **1996**.

Chart 1

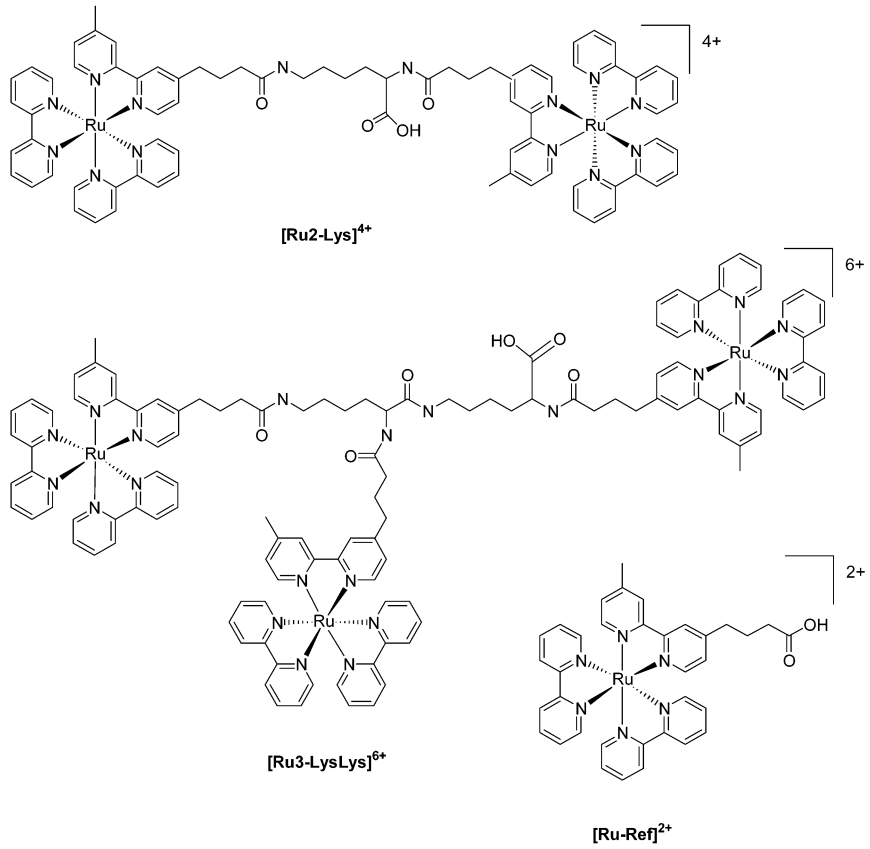

removed under reduced pressure at 40 °C. Purification was performed by preparative HPLC with Millipore water and acetonitrile (both containing TFA, 0.1%) as eluent, following a gradient method (0−40% acetonitrile in 120 min). The collected fractions containing the product were regrouped according to the analytical HPLC retention time and stored, after addition of a saturated aqueous NH_4PF_6 solution, overnight at 4 °C. The precipitate was filtered off, washed with water, and dried under vacuum at 60 °C to give the product as pure orange powder.

Yield: 311 mg (75%). In the NMR assignments, the traditional proton numbering scheme for bpy ligands was used. For the substituted bpy ligands, the two different rings were denoted by symbols a and a′ added behind the number. ^{1}H NMR (CD_2Cl_2): 8.41 (m, 8H, 3), 8.35/8.34 (2s, 4H, 3a + 3a′), 8.03 (m, 8H, 4), 7.64−7.88 (m, 8H, 6), 7.36−7.52 (m, 12H, 5 + 6a + 6a′), 7.25/7.21 (2d, J = 3.3 Hz, 4H, 5a + 5a′), 6.90 (s, 1H, CH(COOH)−N*H*), 6.24 (s, 1H, CH(COOH)−$(CH_2)_4$−N*H*), 4.23 (s, 1H, COOH), 3.65 (m, 1H, C*H*(COOH)), 3.14/3.06 (2 m, 2H, CH(COOH)−$(CH_2)_3$−CH_2), 2.83 (m, 4H, C(O)−CH_2), 2.54 (s, 6H, bpy-CH_3), 2.32/2.22 (2m, 4H, bpy-CH_2), 2.01 (br m, 4H, bpy-CH_2−CH_2), 1.55 (br m, 4H, CH(COOH)−CH_2−CH_2−CH_2), 1.28 (br m, 2H, CH(COOH)−CH_2−CH_2) ppm. ESI-MS: m/z 483.7 [M^+ − $4PF_6$ − H], 362.3 [M^+ − $4PF_6$]. Elemental analysis: $C_{76}H_{74}N_{14}O_4Ru_2P_4F_{24}$ (2029.49); Calcd: C, 44.98; H, 3.68; N, 9.66; found: C, 44.81; H, 3.74; N, 9.68.

[Ru3−LysLys](PF$_6$)$_6$. This compound was synthesized following the same procedure described for **[Ru2−Lys](PF$_6$)$_4$**. N^6-L-lysyl-L-lysine trihydrochloride (29 mg, 0.075 mmol) in phosphate buffer solution (10 mL, pH 8) was added dropwise to [Ru(bpy)$_2$(bpyOSu)](PF$_6$)$_2$ (350 mg, 0.302 mmol) in dimethylformamide (50 mL). The product was obtained as an orange powder. Yield: 105 mg (45%). Proton numbering as for the previous compound. ^{1}H NMR (CD_3CN): 8.48 (m, 12H, 3), 8.39 (m, 6H, 3a + 3a′), 8.04 (m, 12H, 4), 7.71 (m, 12H, 6), 7.53 (m, 6H, 6a + 6a′), 7.39 (m, 12H, 5), 7.23 (m, 6H, 5a + 5a′), 6.97/6.69 (2 t, 1H, NH), 6.44 (m, 2H, NH), 4.24 (br s, 1H, COOH), 3.04 (m, 2H, CH(COOH)−$(CH_2)_3$−CH_2), 2.78 (m, 4H, C(O)−CH_2), 2.52 (s, 6H, bpy-CH_3), 1.5−2.3 (br m, 12H, bpy-CH_2−CH_2 + CH(COOH)−CH_2−CH_2−CH_2), 1.40/1.32 (2 m, 2H, CH(COOH)−CH_2−CH_2) ppm. ESI-MS: m/z 556.7 [M^+ − $6PF_6$ − 2H], 445.7 [M^+ − $6PF_6$ − H]. Elemental analysis: $C_{117}H_{116}N_{22}O_6Ru_3P_6F_{36}$ (3099.32); Calcd: C, 45.34; H, 3.77; N, 9.94; found: C, 45.20; H, 3.88; N, 9.96.

The multinuclear complexes **[Ru2−Dend]**$(PF_6)_4$, **[Ru4−Dend]**$(PF_6)_8$, and **[Ru8−Dend]**$(PF_6)_{16}$[35] were prepared and purified in a similar procedure described for the other multinuclear complexes. **[Ru2−Dend]**$(PF_6)_4$ MS spectra (ES pos. mode): M^{4+} 815.1, MW 3260; **[Ru4−Dend]**$(PF_6)_8$ MS spectra (ES pos. mode): M^{8+} 596.0, MW 4766; **[Ru8−Dend]**$(PF_6)_{16}$ MS spectra (ES pos. mode): M^{10+} 948.0, MW 9487.

General Techniques. Analytical HPLC was performed on a Merck Hitachi apparatus equipped with L 7100 HPLC pump, L 7200 autosampler, L 7400 UV-detector, 3612 ERC Erma degasser, and Vydac C18 (300 Å, 5 μm) column. The setup for preparative HPLC was equipped with a Gynkotek pump (M480P), a Soma detector (S-3710), an Abimed automated fraction collector (M202), and a Vydac C18 (300 Å, 15−20 μm, 50−250 mm) column. Electrospray ionization (ESI) mass spectra were measured on a Platform II (Micromass) spectrometer. Cyclic voltammetry (CV), chronoamperometry, and voltammetry at ultramicroelectrode (UME) were performed with a gastight single-compartment cell under an atmosphere of dry nitrogen or argon. For conventional CV and chronoamperometry, the cell was equipped with Pt disk working (apparent surface area of 0.42 mm^2), Pt wire auxiliary, and Ag wire pseudoreference electrodes. The working electrode was carefully

Chart 2

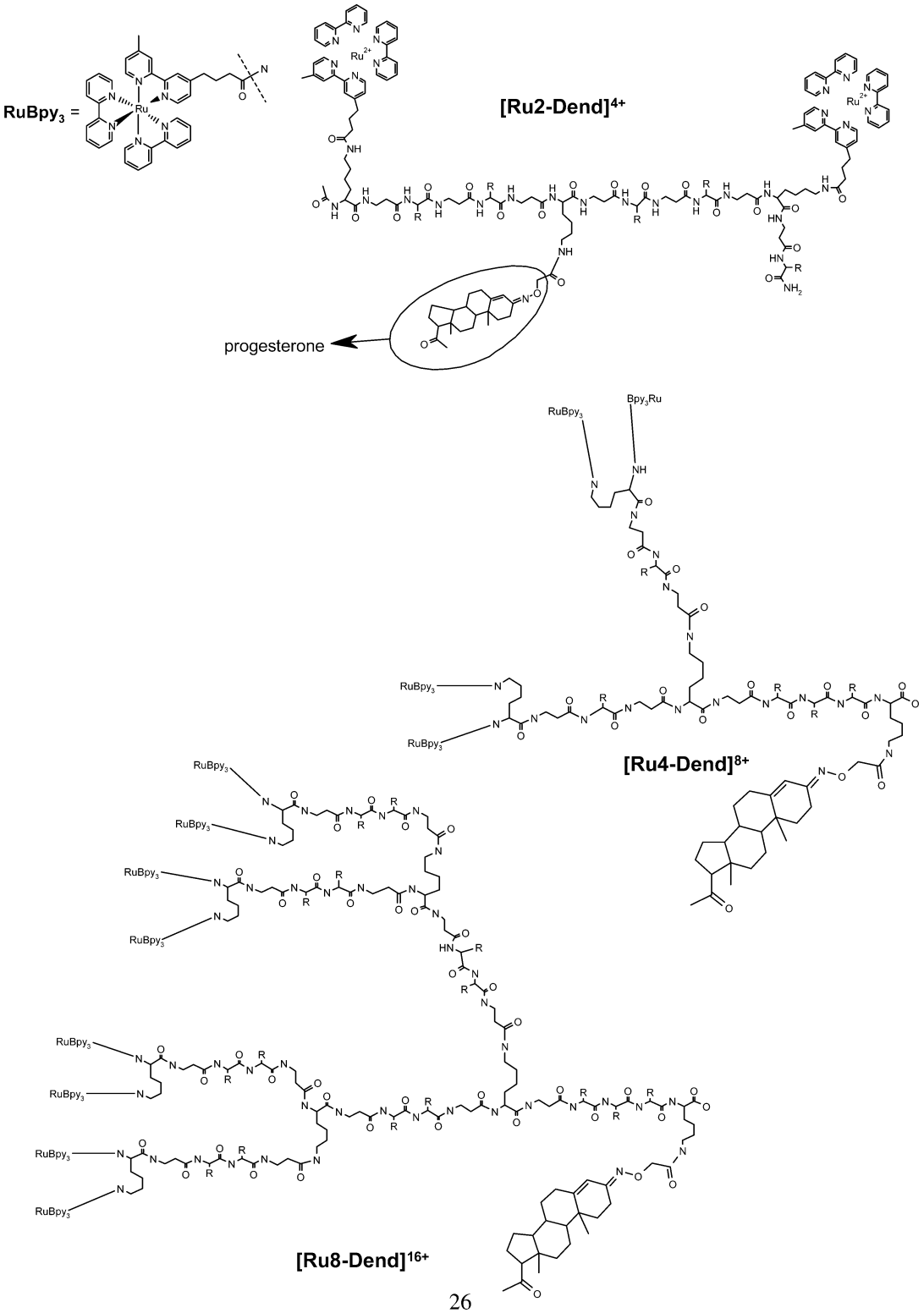

polished with a 0.25 μm-grain diamond paste between scans. The working ultramicroelectrode (UME) was a homemade $d = 10$ μm Pt disk. The potential control was achieved with a PAR model 283 potentiostat. For chronoamperometry, the potential was stepped from a value typically 100−300 mV less positive than the oxidation potential of the complex to a value 100−300 mV more positive. All redox potentials are reported against the ferrocene-ferrocenium (Fc/Fc^+) redox couple used as an internal standard[36] ($E°_{1/2} = +0.63$ V vs NHE).[37] Ferrocene also served as the standard for the number of electrons (n_{app}) exchanged at the electrode and the diffusion coefficient (D), determination ($n_{app(Fc)} = 1$ and $D_{(Fc)} = 1.9 \times 10^{-5}$ $cm^2\ s^{-1}$ in acetonitrile).[38] The acetonitrile solutions of ca. 4×10^{-4} M complex were prepared under nitrogen. Bu_4NPF_6 (10^{-1} M) was used as supporting electrolyte.

(36) Gritzner, G.; Kůta, J. *Pure Appl. Chem.* **1984**, *56*, 461−466.

Table 1. Electrochemical Data for the Investigated Complexes and Reference Compounds[a]

	$Ru^{II/III}$	$bpy^{0/-1}$	n_{app}[b]	D[c] (10^5 cm^2 s^{-1})
[Ru−Ref]$^{2+}$	+0.84	−1.74	1.1 ± 0.1	1.10 ± 0.06
		−1.96		
[Ru2−Lys]$^{4+}$	+0.83	−1.74	1.8 ± 0.1	0.64 ± 0.03
		−1.88		
[Ru3−LysLys]$^{6+}$	+0.86	−1.74	3.4 ± 0.3	0.34 ± 0.03
		−1.81		
$[Ru(bpy)_3]^{2+}$	+0.89	−1.72		
		−1.93		
$[Ru(bpy)_2$(4-octoxy-bpy)$]^{2+}$ [d]	+0.75[e]	−1.82[e]		1.05

[a] Redox potentials ($E_{1/2}$) in volts vs Fc/Fc^+, in acetonitrile at 293 K. [b] Number of electrons transferred during the oxidation. [c] Diffusion coefficient. [d] Reference 25. [e] $E_{1/2}(Fc/Fc^+) = 0.421$ V vs Ag/AgCl in acetonitrile.[50]

UV−vis spectra were recorded on a Hewlett-Packard 8453 diode-array spectrophotometer. Emission spectra were recorded on a Spex 1681 spectrophotometer. All emission spectra were corrected for the photomultiplier response.

ECL studies were performed using an Elecsys instrument (Roche Diagnostics GmbH).[39] It consists of an automated system for handling the solutions, a flow-through chamber cell, a potentiostat, and a red-light-sensitive photomultiplier tube, placed above an optically transparent window of the cell. The cell was equipped with a sheet platinum working electrode (4.8 mm × 5.0 mm) and a platinum auxiliary electrode made of two wires symmetrically placed above the working electrode. As reference, an Ag/AgCl (KCl-saturated) electrode was employed. Solutions for ECL homogeneous assays were prepared in phosphate buffer (3×10^{-1} M phosphate salt in deionized water) containing 1.8×10^{-1} M TPrA. The pH value was adjusted to 6.8 with NaOH or H_3PO_4 aqueous solutions. Nonionic surfactant was added, when required, in amounts above its critical micellar concentration (cmc). Solutions were 10^{-8} M in ruthenium units for **[Ru−Ref]$^{2+}$**, **[Ru2−Lys]$^{4+}$**, and **[Ru3−LysLys]$^{6+}$**, and 10^{-8} M in the complex for **[Ru2−Dend]$^{4+}$**, **[Ru4−Dend]$^{8+}$**, and **[Ru8−Dend]$^{16+}$**. Solutions for ECL heterogeneous progesterone immunoassays contained (3.2×10^{-10} M) multimetallic complex, (3.2×10^{-10} M) biotin antibody conjugates, streptavidin-coated nanoparticles with biotin-binding capacity of 2.4×10^{-4} mol dm^{-3}, (1.8×10^{-1} M) TPrA, and a nonionic surfactant. For **[Ru8−Dend]$^{16+}$** solutions were 1.6×10^{-10} M in the multimetallic complex and 1.6×10^{-10} M in biotin antibody conjugates. Solutions for heterogeneous assays were measured after a few minutes of incubation time. Estimated experimental error for the reported ECL intensities is 5%.

Results and Discussion

Electrochemistry. The electrochemical data for the investigated complexes **[Ru2−Lys]$^{4+}$**, **[Ru3−LysLys]$^{6+}$**, and the reference compounds **[Ru−Ref]$^{2+}$** [33,34] and $[Ru(bpy)_3]^{2+}$ [40,41] in acetonitrile solution are summarized in Table 1. The redox behavior of the bi- and trinuclear compounds is consistent with predominantly metal-based oxidation and ligand-based reductions, in agreement with literature data for several related multinuclear complexes.[42,43]

The oxidation of **[Ru2−Lys]$^{4+}$** and **[Ru3−LysLys]$^{6+}$** occurs in a single reversible two- and three-electron step (see below) at potentials $E_{1/2} = +0.83$ and +0.86 V, respectively, that are very close to those obtained for the reference **[Ru−Ref]$^{2+}$** and $[Ru(bpy)_3]^{2+}$ ($E_{1/2} = +0.84$ and +0.89 V, respectively).

In the cathodic region, **[Ru2−Lys]$^{4+}$** and **[Ru3−LysLys]$^{6+}$** exhibit the first multielectron (two- and three-electron, respectively; see below) reversible wave at the same potential as **[Ru−Ref]$^{2+}$** ($E_{1/2} = -1.74$ V), close to the value found for $[Ru(bpy)_3]^{2+}$ (−1.72 V). This step most likely corresponds to the unresolved reduction of the ancillary 2,2′-bipyridines, one at each Ru(II) center, that are better electron acceptors than the alkyl-substituted bipyridine ligands.[44] At more negative potentials, the reduced di- and trinuclear complexes **[Ru2−Lys]$^{2+}$** and **[Ru3−LysLys]$^{3+}$** undergo second multielectron reduction process, with a sharp peak developed along the corresponding reoxidation step due to adsorption of the neutral species **[Ru2−Lys]** and **[Ru3−LysLys]** on the cathode. The reduction potentials are $E_{1/2} = -1.88$ and −1.81 V, respectively, i.e., less negative than those found for the reference **[Ru−Ref]$^{2+}$** and $[Ru(bpy)_3]^{2+}$ (−1.96 and −1.93 V, respectively). The second cathodic process is assigned to the reduction of the remaining neutral ancillary 2,2′-bipyridine ligands at each Ru(II) center. Further reductions could not be readily observed due to strong adsorption of the neutral products. Application of a glassy carbon disk electrode did not improve the voltammetric record.

The peak currents of the first and second cathodic steps are similar to that of the Ru(II)/Ru(III) anodic peak, consistent with the identical number of electrons exchanged. The poor resolution of the multielectron anodic and cathodic waves proves weak electronic communication between the metal centers and the remote ancillary 2,2′-bipyridine ligands, respectively.

For **[Ru2−Lys]$^{4+}$**, **[Ru3−LysLys]$^{6+}$**, and the reference complex **[Ru−Ref]$^{2+}$**, the number of electrons exchanged at the electrode surface during the oxidation step (n_{app}) and the diffusion coefficient (D) were separately determined, following the convenient literature procedure reported by Amatore et al.[38,45,46]

The values of n_{app} and D determined for **[Ru−Ref]$^{2+}$**, **[Ru2−Lys]$^{4+}$**, and **[Ru3−LysLys]$^{6+}$** in acetonitrile are reported in Table 1. As expected, the number of electrons transferred (1.1 ± 0.1, 1.8 ± 0.1, and 3.4 ± 0.3, respectively) in the oxidation process of the three complexes is proportional to the number of the poorly communicating metal centers that oxidize at the same potential. The diffusion coefficients (D) are (1.10 ± 0.06) × 10^{-5}, (0.64 ± 0.03) ×

(37) Pavlishchuk, V. V.; Addison, A. W. *Inorg. Chim. Acta* **2000**, *298*, 97−102.
(38) Rossenaar, B. D.; Hartl, F.; Stufkens, D. J.; Amatore, C.; Maisonhaute, E.; Verpeaux, J.-N. *Organometallics* **1997**, *16*, 4675−4685.
(39) Erler, K. *Wien. Klin. Wochenschr.* **1998**, *110*, 5−10.
(40) Paris, J. P.; Brandt, W. W. *J. Am. Chem. Soc.* **1959**, *81*, 5001.
(41) Sutin, N.; Creutz, C. *Adv. Chem. Ser.* **1978**, *168*, 1.
(42) Balzani, V.; Juris, A.; Venturi, M.; Campagna, S.; Serroni, S. *Chem. Rev.* **1996**, *96*, 759−833.
(43) De Cola, L.; Belser, P. *Coord. Chem. Rev.* **1998**, *177*, 301−346.
(44) Elliott, C. M.; Hershenhart, E. J. *J. Am. Chem. Soc.* **1982**, *104*, 7519−7526.
(45) Amatore, C.; Azzabi, M.; Calas, P.; Jutand, A.; Lefrou, C.; Rollin, Y. *J. Electroanal. Chem.* **1990**, *288*, 45−63.

Table 2. UV/Vis Absorption, Luminescence, and ECL Data of the Investigated Complexes and the Reference Compound[a]

	absorption	luminescence				ECL[b]	
	λ_{max} (nm) ϵ (10^{-4} M^{-1} cm^{-1})	λ_{max} (nm)	$\lambda_{max}{}^{c}$ (nm)	ϕ_{em}	$\phi_{em}{}^{c}$	$I_{ecl,rel}$	$I_{ecl,rel}{}^{c}$
[Ru−Ref]$^{2+}$	456 (1.40)	616	617			1	1
[Ru2−Lys]$^{4+}$	456 (2.61) 286 (14.8)	617	616	0.027	0.030	0.80	0.66
[Ru3−LysLys]$^{6+}$	456 (4.29) 286 (24.0)	619	618	0.029	0.030	0.60	0.44

[a] In phosphate buffer solution (3×10^{-1} M, pH 6.8). [b] In the presence of 1.8×10^{-1} M TPrA. [c] In the presence of nonionic surfactant.

10^{-5}, and $(0.34 \pm 0.03) \times 10^{-5}$ cm^2 s^{-1} for **[Ru−Ref]$^{2+}$**, **[Ru2−Lys]$^{4+}$**, and **[Ru3−LysLys]$^{6+}$**, respectively. The D value for **[Ru−Ref]$^{2+}$** is in good agreement with that reported in the literature for a similar Ru(II) complex, [Ru(bpy)$_2$(4-octoxy-2,2′-bipyridine)](PF$_6$)$_2$ in deuterated acetonitrile ($D = 1.05 \times 10^{-5}$ cm^2 s^{-1}).[25] Its decrease in the series **[Ru−Ref]$^{2+}$**, **[Ru2−Lys]$^{4+}$**, and **[Ru3−LysLys]$^{6+}$** is consistent with the increasing size due to the increasing number of metal units of the complexes.

UV−Vis Absorption and Emission. The spectroscopic data for the complexes **[Ru2−Lys]$^{4+}$** and **[Ru3−LysLys]$^{6+}$** are summarized in Table 2. The reference compound **[Ru−Ref]$^{2+}$** is also reported for comparison. In all cases the data refer to aqueous phosphate buffer solutions (pH 6.8). The absorption spectra of **[Ru2−Lys]$^{4+}$** and **[Ru3−LysLys]$^{6+}$** and the emission spectrum of **[Ru3−LysLys]$^{6+}$** in phosphate buffer solutions are depicted in Figure 1.

The UV−vis spectra of **[Ru2−Lys]$^{4+}$** and **[Ru3−LysLys]$^{6+}$** are similar to that of **[Ru−Ref]$^{2+}$**. They exhibit an intense band in the UV region due to intraligand (IL) $\pi-\pi^*$(bpy) transitions and by a broad band in the visible region due to spin allowed dπ (Ru) → π^*(bpy) metal-to-ligand charge-transfer (^{1}MLCT) transitions (Figure 1 and Table 2). The absorption bands do not shift in the series **[Ru−Ref]$^{2+}$**, **[Ru2−Lys]$^{4+}$**, and **[Ru3−LysLys]$^{6+}$**, and the molar absorbance of the di- and trinuclear complexes is proportional to the number of chromophores: about 2- and 3-fold, respectively, that of the mononuclear compound (Table 2). This result is again consistent with the absence of a strong electronic interaction between the chromophores in the multinuclear complexes **[Ru2−Lys]$^{4+}$** and **[Ru3−LysLys]$^{6+}$**.

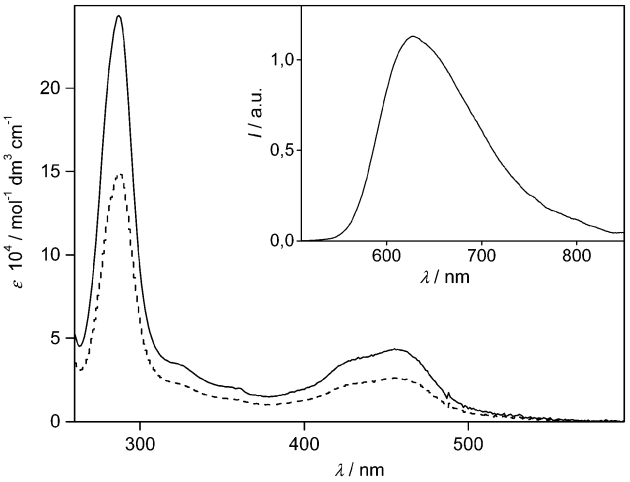

Figure 1. UV−vis absorption spectra of **[Ru3−LysLys]$^{6+}$** (−−−−) and **[Ru2−Lys]$^{4+}$** (− − − −) in phosphate buffer solution. Inset: emission spectrum of **[Ru3−LysLys]$^{6+}$** in phosphate buffer solution at room temperature.

Room-temperature emission spectra of **[Ru−Ref]$^{2+}$**, **[Ru2−Lys]$^{4+}$**, and **[Ru3−LysLys]$^{6+}$** in phosphate buffer solution show nearly identical emission maxima, centered at 616, 617, and 619 nm, respectively (Figure 1 and Table 2). The emitting ^{3}MLCT excited state is therefore the same for all three complexes and lies at the same energy, suggesting that the linkage of several chromophores by the amino acid (Lys) or the dipeptide (LysLys) has negligible effect on their electronic properties, as already deduced from the redox data. The luminescence quantum yields are also very similar for **[Ru2−Lys]$^{4+}$** and **[Ru3−LysLys]$^{6+}$**, viz. 0.027 and 0.029, respectively.

The spectroscopic properties were also investigated for **[Ru−Ref]$^{2+}$**, **[Ru2−Lys]$^{4+}$**, and **[Ru3−LysLys]$^{6+}$** in phosphate buffer solutions containing a nonionic surfactant above its critical micellar concentration (cmc). Upon addition of surfactant, UV−vis and emission spectra reveal only minor changes, with emission maxima at 617, 616, and 618 nm for **[Ru−Ref]$^{2+}$**, **[Ru2−Lys]$^{4+}$**, and **[Ru3−LysLys]$^{6+}$**, re-

(46) For the measurement of the number of electrons (n_{app}) exchanged at the electrode and the diffusion coefficient (D), transient chronoamperometry and steady-state voltammetry at an ultramicroelectrode (UME) were combined to provide two independent equations for the faradic current, i, as a function of the two independent variables n_{app} and D.[44] A standard compound (ferrocene) with known n_{app} and D is employed to avoid errors arising from the determination of the surface area of the planar disk electrode used in chronoamperometry technique.[37,44] For the ferrocene/analyte system the following equations apply:

$$n_{app} = n_{app(Fc)}[R_{chrono}{}^2/R_{UME}] \quad (2)$$

$$D = D_{(Fc)}[R_{chrono}/R_{UME}]^2 \quad (3)$$

where R_{chrono} and R_{UME} are expressed as

$$R_{chrono} = [ic_{0(Fc)}]/[i_{(Fc)}c_0] \quad (4)$$

$$R_{UME} = [i_{lim}c_{0(Fc)}]/[i_{lim(Fc)}c_0] \quad (5)$$

In eqs 4 and 5, c_0 is the bulk concentration of the analyte, i is chronoamperometric current response at the duration time t of the potential step, and i_{lim} is the limiting value for the current in the steady-state voltammetry at UME. n_{app} is a function of the characteristic time (T_c) of the technique used, and in other terms of the time needed by a molecule to cross the diffusion layer at the electrode surface, it is necessary to perform the measurements using the same T_c value for both the two techniques. In chronoamperometry, T_c is the duration time t of the potential step, while in steady-state voltammetry at the disk UME T_c is given by $r_0{}^2D^{-1}$, where r_0 is the radius of the UME. On the grounds of the values of $D_{(Fc)}$ and r_0 of the UME employed, T_c for the ferrocene was estimated to be 53 ms. R_{chrono} was then determined for the investigated complexes as the average between different duration times t within the range of 15−300 ms, and for each experiment it was checked that T_c, calculated using the experimental value of D, was falling within the range of the t values considered in the chronoamperometric measurements.

spectively, and quantum yields of 0.030 for both **[Ru2−Lys]**$^{4+}$ and **[Ru3−LysLys]**$^{6+}$. Formation of complex micelle aggregations in the presence of the nonionic surfactant Triton X-100 was observed for some methyl- and phenyl-substituted phenanthroline ruthenium complexes, resulting in strong emission changes, viz. red-shift of the emission maxima, higher emission quantum yields, and longer excited-state lifetimes.[47,48] However, $[Ru(bpy)_3]^{2+}$ does not exhibit pronounced changes of the emission due to the weak hydrophobic interactions between the 2,2′-bipyridine ligands and the hydrophobic cavity of the micelles.[47,48] The behavior of **[Ru2−Lys]**$^{4+}$ and **[Ru3−LysLys]**$^{6+}$ closely resembles that of $[Ru(bpy)_3]^{2+}$, with the bipyridine ligands only weakly interacting with the surfactant.

Electrochemiluminescence. The electrochemical and spectroscopic studies have shown a very weak, if any, electronic interaction among the ruthenium units in the multimetallic compounds that therefore behave as **[Ru−Ref]**$^{2+}$. This is an important requirement when more metal centers are linked by a bridging ligand to increase a specific output, in this case emission, as the sum of the single-unit contributions.

We aimed at investigating the ECL behavior of **[Ru2−Lys]**$^{4+}$ and **[Ru3−LysLys]**$^{6+}$ in phosphate buffer solution with added tri-*n*-propylamine (TPrA) as co-reactant. In a simplified description of the ECL mechanism,[11,15,16,19,24] the $[Ru(bpy)_3]^{2+}$ units are oxidized to $[Ru(bpy)_3]^{3+}$ and, simultaneously, TPrA molecules to the radical cations $Pr_2N^{\bullet+}CH_2$-CH_2CH_3 that form the radical species $Pr_2NC^{\bullet}HCH_2CH_3$ upon loss of an α-proton. The radical $Pr_2NC^{\bullet}HCH_2CH_3$ concomitantly reduces $[Ru(bpy)_3]^{3+}$ to $*[Ru(bpy)_3]^{2+}$ in the excited state and converts irreversibly into $Pr_2N^{+}{=}CHEt$ (eq 1). Excited $*[Ru(bpy)_3]^{2+}$ decays with visible light emission to the ground state.

$$[Ru(bpy)_3]^{3+} + Pr_2NC^{\bullet}HCH_2CH_3 \rightarrow *[Ru(bpy)_3]^{2+} + Pr_2N^{+}{=}CHEt \quad (1)$$

For the ECL measurements, the solutions of **[Ru2−Lys]**$^{4+}$, **[Ru3−LysLys]**$^{6+}$, and reference **[Ru−Ref]**$^{2+}$ in phosphate buffer were equivalent in concentration of the ruthenium moieties and contained TPrA in a large excess (>10^6-fold the concentration of the complexes). A nonionic surfactant was also added to investigate the ECL behavior of the multinuclear complexes under the same experimental conditions as applied in routine immunoassays in diagnostics. In automated immunoassay analyzers,[39] surfactants are employed to achieve a good liquid flow, to avoid formation of bubbles, and to better remove the analyte from the ECL cell after each measurement. Furthermore, surfactants increase the solubility of the hydrophobic ruthenium polypyridyl complexes in aqueous solutions.[23] The ECL signals of **[Ru−Ref]**$^{2+}$, **[Ru2−Lys]**$^{4+}$, and **[Ru3−LysLys]**$^{6+}$ were recorded against time over a range of 700 ms after triggering the reaction (Figure 2). The ECL results are given in Table 2 as intensity integrals relative to **[Ru−Ref]**$^{2+}$ ($I_{ecl,rel} = 1$) calculated per ruthenium unit. The data are averaged over six trials.

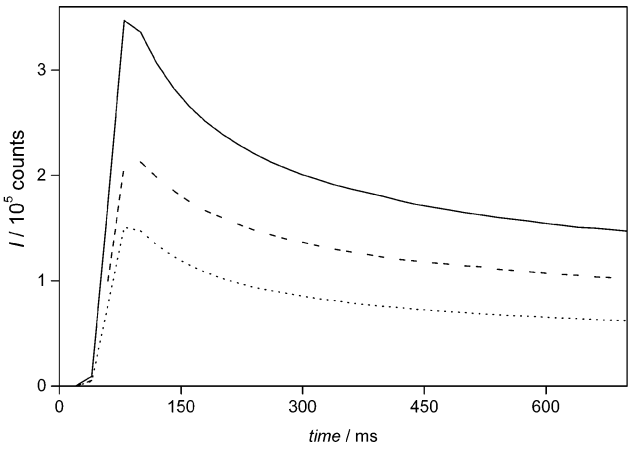

Figure 2. ECL of **[Ru−Ref]**$^{2+}$ (—), **[Ru2−Lys]**$^{4+}$ (− − − −), and **[Ru3−LysLys]**$^{6+}$(····) in phosphate buffer solution containing TPrA and surfactant.

The ECL signals of **[Ru−Ref]**$^{2+}$, **[Ru2−Lys]**$^{4+}$, and **[Ru3−LysLys]**$^{6+}$ increase sharply within a few milliseconds after triggering the reaction, decaying slowly afterward (Figure 2). The initial sharp peak is due to the presence of the ruthenium complexes and TPrA molecules close to the electrode surface, which readily oxidize. The consumption of the active species in the proximity of the anode and their slow diffusion from the bulk solution result in decreased signal intensity. Passivation of the anodic surface due to the formation of PtO_x may also contribute to the signal decay. Surprisingly, the ECL intensity monitored at the signal maximum decreases in the series **[Ru−Ref]**$^{2+}$, **[Ru2−Lys]**$^{4+}$, and **[Ru3−LysLys]**$^{6+}$. This behavior is not completely clear, since one would expect similar initial response for all three complexes, the concentration of the active species at the anodic surface being initially the same. These differences most likely arise due to different adsorption of the complexes at the electrode.

The relative intensities per ruthenium unit of **[Ru2−Lys]**$^{4+}$ and **[Ru3−LysLys]**$^{6+}$ are 0.66 and 0.44, respectively (Table 2). Some decrease of the ECL signal in the series **[Ru−Ref]**$^{2+}$, **[Ru2−Lys]**$^{4+}$, and **[Ru3−LysLys]**$^{6+}$ is expected, in accordance with the decreasing diffusion coefficients (1.1, 0.65, and 0.33×10^{-5} cm^2 s^{-1}, respectively). However, on the grounds of the diffusion coefficients, the relative ECL intensities per ruthenium unit are estimated to be ca. 0.8 and 0.5 for **[Ru2−Lys]**$^{4+}$ and **[Ru3−LysLys]**$^{6+}$, respectively, as the faradaic current is proportional to $D^{1/2}$. Hence, the experimental values are lower than expected. To investigate whether this discrepancy is due to a less efficient reaction between the multinuclear complexes and the radical species generated upon oxidation of TPrA or due to some effects caused by the surfactant, the ECL measurements were also performed in a surfactant-free phosphate buffer solution. In this case, almost no ECL signal could be detected. This result points to a crucial role played by detergents in the ECL measurements. Recent studies have shown that protec-

(47) Mandal, K.; Hauenstein, B. L., Jr.; Demas, J. N.; DeGraff, B. A. *J. Phys. Chem.* **1983**, *87*, 328−331.
(48) Dressick, W. J.; Hauenstein, B. L., Jr.; Gilbert, T. B.; Demas, J. N.; DeGraff, B. A. *J. Phys. Chem.* **1984**, *88*, 3337−3340.

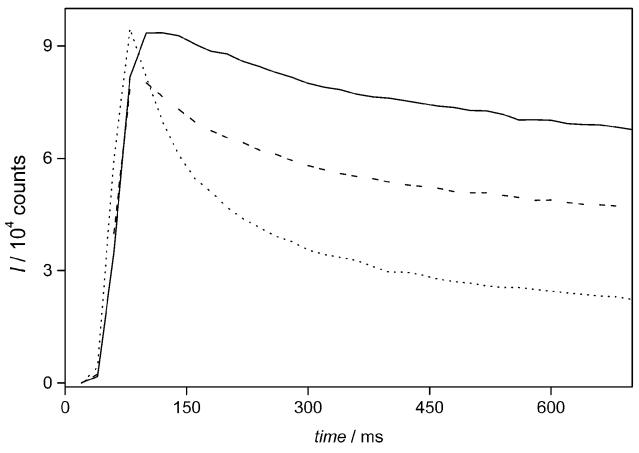

Figure 3. ECL of **[Ru−Ref]**$^{2+}$ (—), **[Ru2−Lys]**$^{4+}$ (− − − −), and **[Ru3−LysLys]**$^{6+}$(····) in the phosphate buffer solution containing TPrA, in the absence of surfactant.

tion of the electrode surface from passivation, for instance, upon addition of halides (e.g., Br^-, I^-) to the assay buffer solution, greatly enhances the current due to the oxidation of TPrA and the ECL signal of the TPrA/$[Ru(bpy)_3]^{2+}$ system.[15] Enhancement of the anodic current and ECL output was also observed when increasing the hydrophobicity of the electrode surface, e.g., upon formation of a layer of alkanethiols or nonionic surfactant (Triton X-100) on the electrode.[16] It has been suggested that the hydrophobic interaction of the TPrA molecules with the electrode surface promotes their closer approach to the electrode, thereby facilitating the electron-transfer reaction.[16] Hence, the presence of surfactant can be important for two reasons: to protect the electrode from passivation and to facilitate the oxidation of the active species.

ECL measurements were then performed with **[Ru−Ref]**$^{2+}$, **[Ru2−Lys]**$^{4+}$, and **[Ru3−LysLys]**$^{6+}$ in phosphate buffer after having washed the cell with a solution containing a nonionic surfactant (Thesit, poly(ethylene glycol) 400 dodecyl ether, 0.1%). This step led to formation of a hydrophobic layer on the electrode surface prior to the measurement.[16] The solutions of the investigated complexes were again equivalent in the concentration of the ruthenium units and contained an excess of TPrA. The ECL intensities are reported in Table 2, and the signals are plotted against time in Figure 3.

The presence of surfactant in the washing buffer solution resulted in a dramatic increase of the ECL signal, compared to the measurements performed in its absence. The ECL profiles reach a maximum within a few milliseconds after application of a positive potential, with similar peak maxima for the three complexes, and decay slowly afterward (Figure 3). Importantly, the relative ECL intensities per ruthenium unit are 0.80 and 0.60 (Table 2) for **[Ru2−Lys]**$^{4+}$ and **[Ru3−LysLys]**$^{6+}$, respectively, in good agreement with the values estimated on the grounds of the diffusion coefficients (0.8 and 0.5, respectively). These results suggest that the differences between the ECL intensities of **[Ru−Ref]**$^{2+}$, **[Ru2−Lys]**$^{4+}$, and **[Ru3−LysLys]**$^{6+}$, recorded when using surfactant only prior to the measurements, can easily be explained with the different diffusion rates of the complexes. There was no evidence found for a different reactivity of the three complexes with the active TPrA species.

The presence of a layer of surfactant on the electrode surface is then important to have intense ECL signal. However, its addition to the ruthenium complex solution above the cmc value slightly decreases the ECL signal intensity. In this case, **[Ru−Ref]**$^{2+}$ shows a signal that corresponds to 80% of that recorded when surfactant is only added to the washing solution and used prior to the measurements. Furthermore, the relative intensities for the complexes **[Ru2−Lys]**$^{4+}$ and **[Ru3−LysLys]**$^{6+}$ are lower (0.66 and 0.44, respectively) when surfactant is used in the ruthenium complex solution (see above). The spectroscopic properties of the investigated compounds have shown no dependence on the surfactant. The reduced ECL response must therefore depend on other factors. It was reported that, despite the weak interaction between $[Ru(bpy)_3]^{2+}$ and micelles of nonionic surfactant, a different diffusion coefficient is found for $[Ru(bpy)_3]^{2+}$ in water ($D = 7.33 \times 10^{-8}$ cm^2 s^{-1}) and in aqueous solution containing the surfactant Triton X-100 ($D = 4.70 \times 10^{-8}$ cm^2 s^{-1}).[49] A similar effect can be expected for the complexes **[Ru−Ref]**$^{2+}$, **[Ru2−Lys]**$^{4+}$, and **[Ru3−LysLys]**$^{6+}$, resulting in smaller diffusion coefficients when surfactant is added to the assay buffer solutions, thereby explaining the lower ECL intensity observed. Another possibility could be the quenching of the excited ruthenium unit by a nearby oxidized ruthenium moiety, if not all the oxidized units are reduced to the excited state or decay to the ground state. In such a case, an electron transfer from the excited ruthenium species to the oxidized unit could occur, resulting in an emission quenching.

As shown by these ECL measurements, the diffusion rates are most likely the limiting factor for the improvement of the ECL intensity of the investigated complexes, **[Ru2−Lys]**$^{4+}$ and **[Ru3−LysLys]**$^{6+}$. However, as the ECL intensities considered so far are calculated per individual ruthenium unit (0.66 and 0.44 in the presence of surfactant in the assay buffer), equimolar concentrations of the multimetallic complexes yield relative intensities of 1.32 for both **[Ru2−Lys]**$^{4+}$ and **[Ru3−LysLys]**$^{6+}$, hence resulting in an increase of ca. 30% with respect to mononuclear reference **[Ru−Ref]**$^{2+}$.

ECL Immunoassay. In the research laboratories of Roche Diagnostics GmbH, large dendritic peptidic structures have been developed containing two, four, and eight $[Ru(bpy)_3]^{2+}$ moieties, viz. **[Ru2−Dend]**$^{4+}$, **[Ru4−Dend]**$^{8+}$, and **[Ru8−Dend]**$^{16+}$, respectively.[35] Their molecular structures are depicted in Chart 2. The multinuclear complexes were bound to a modified progesterone molecule via a peptidic bond,[35] and their ECL behavior was investigated. Furthermore, they were tested in heterogeneous ECL-based progesterone immunoassays.

For the ECL investigations, the solutions of **[Ru2−Dend]**$^{4+}$, **[Ru4−Dend]**$^{8+}$, and **[Ru8−Dend]**$^{16+}$ in phosphate

(49) Workman, S.; Richter, M. M. *Anal. Chem.* **2000**, *72*, 5556−5561.
(50) Sinclair, L.; Mondal, J. V.; Uhrhammer, D.; Schultz, F. A. *Inorg. Chim. Acta* **1998**, *278*, 1.

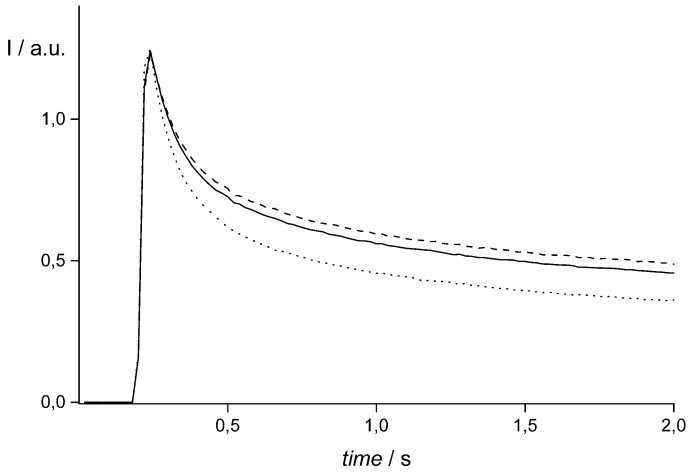

Figure 4. ECL of **[Ru2−Dend]**$^{4+}$ (—), **[Ru4−Dend]**$^{8+}$ (− − − −), and **[Ru8−Dend]**$^{16+}$(····) in phosphate buffer solution containing TPrA and nonionic surfactant.

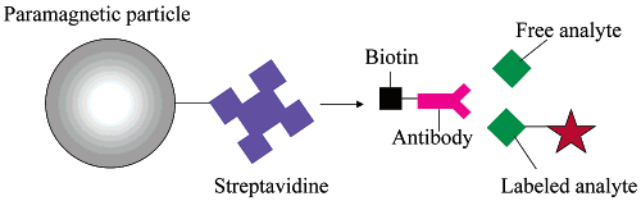

Figure 5. Scheme of a competitive heterogeneous immunoassay.

buffer were equivalent in concentration of the multimetallic complex and contain a large excess of TPrA. A nonionic surfactant was also added to perform the measurements under the same experimental conditions as employed for routine progesterone immunoassays. The ECL signals recorded for **[Ru2−Dend]**$^{4+}$, **[Ru4−Dend]**$^{8+}$, and **[Ru8−Dend]**$^{16+}$ against time are depicted in Figure 4. The signal profiles are similar to those of the smaller **[Ru−Ref]**$^{2+}$, **[Ru2−Lys]**$^{4+}$, and **[Ru3−LysLys]**$^{6+}$ complexes, with a sharp peak occurring within a few milliseconds, after triggering the reaction, followed by a slow decrease. The intensity integrals do not differ much for the three complexes, the absolute values being 43 400, 45 500, and 36 422 counts, respectively. As for **[Ru2−Lys]**$^{4+}$ and **[Ru3−LysLys]**$^{6+}$ (see above), slower diffusion probably plays an important role in limiting the enhancement of the ECL intensity upon increase of the number of ruthenium centers and size of the complex.

The compounds **[Ru2−Dend]**$^{4+}$, **[Ru4−Dend]**$^{8+}$, and **[Ru8−Dend]**$^{16+}$ were then tested in ECL-based progesterone immunoassays employing paramagnetic nanoparticle technology.[14,39]

In this technology, the immunoassay is performed on streptavidin-coated paramagnetic particles (heterogeneous assay), by linking the antibody specific for progesterone to a biotin molecule that is able to strongly interact with the streptavidin via noncovalent bindings (Figure 5). Prior to triggering the reaction, the assay buffer solution containing streptavidin-coated nanoparticles, biotin antibody conjugates, and progesterone molecules labeled with the multinuclear ruthenium complex is allowed to incubate for a few minutes and drawn afterward into the electrochemical cell. The nanoparticles are then captured on the surface of the working

Table 3. ECL Progesterone Immunoassay Data for **[Ru2−Dend]**$^{4+}$, **[Ru4−Dend]**$^{8+}$, and **[Ru8−Dend]**$^{16+}$ Complexes[a]

progesterone (10^9 mol dm^{-3})	ECL		
	[Ru2−Dend]$^{4+}$	**[Ru4−Dend]**$^{8+}$	**[Ru8−Dend]**$^{16+}$ [b]
0	43111	99583	78021
0.175	40053	90049	64555
1.75	26212	65779	55863
6×10^4	2361	14791	40130

[a] Data are given as absolute intensity integrals for solutions in phosphate buffer (3×10^{-1} M, pH 6.8) containing (3.2×10^{-10} M) multimetallic complex, (3.2×10^{-10} M) biotin antibodies, and streptavidin-coated nanoparticles with 2.4×10^{-4} M biotin-binding capacity. Solutions also contained 1.8×10^{-1} M TPrA and nonionic surfactant. [b] 1.6×10^{-10} mol dm^{-3}, with (1.6×10^{-10} M) biotin antibodies.

electrode by means of a magnet placed underneath. Unbound species can be then removed upon washing the cell with a buffer solution containing the TPrA molecules. Besides the possibility to separate bound from unbound species, the nanoparticle technology also has the advantage of collecting the ECL reactive ruthenium centers on the working electrode, hence ensuring that a large proportion of ruthenium labels is accessible for ECL reaction.

The progesterone immunoassays for **[Ru2−Dend]**$^{4+}$, **[Ru4−Dend]**$^{8+}$, and **[Ru8−Dend]**$^{16+}$ were performed by a competitive mechanism (Figure 5) where the analyte (free progesterone) competes with the labeled progesterone for the binding site of the antibodies. The solution containing the labeled progesterones, the biotin antibody conjugates, and the streptavidin-coated nanoparticles was titrated with increasing concentrations of the analyte, and the ECL signal was recorded. Solutions of **[Ru2−Dend]**$^{4+}$, **[Ru4−Dend]**$^{8+}$, and **[Ru8−Dend]**$^{16+}$ in phosphate buffer were equimolar for **[Ru2−Dend]**$^{4+}$ and **[Ru4−Dend]**$^{8+}$ and half concentrated for **[Ru8−Dend]**$^{16+}$. They contained TPrA in a large excess, together with a nonionic surfactant.

In the absence of the free progesterone, the ECL intensity integrals calculated for **[Ru2−Dend]**$^{4+}$, **[Ru4−Dend]**$^{8+}$, and **[Ru8−Dend]**$^{16+}$ are 43 100, 99 600, and 78 000 counts, respectively (Table 3). They are then proportional to the number of the ruthenium units present in the complex, considering that **[Ru8−Dend]**$^{16+}$ was half concentrated with

respect to **[Ru2−Dend]**$^{4+}$ and **[Ru4−Dend]**$^{8+}$. Upon addition of progesterone, the ECL intensity decreases, as the analyte competes with the labeled progesterone for the binding site of the antibodies. For a large excess of the analyte (>100-fold the concentration of the complex), the ECL of **[Ru2−Dend]**$^{4+}$ drops to 5% of the initial signal, consistent with the strong competition of the analyte present in solution (Table 3). This residual ECL (background) signal increases moderately for **[Ru4−Dend]**$^{8+}$ (10%) and dramatically for **[Ru8−Dend]**$^{16+}$ (46%) (Table 3). The high background ECL signal observed for **[Ru4−Dend]**$^{8+}$ and, in particular, for **[Ru8−Dend]**$^{16+}$ is most probably due to nonspecific binding of the multimetallic complexes to the streptavidin-coated nanoparticles or to the large antibodies, via strong hydrophobic interactions.

These immunoassay results show that upon increasing the number of ruthenium units bound to the dendritic structure that labels a biological molecule (e.g., antigen, antibody), the ECL signal can be proportionally enhanced. Because in heterogeneous assays where nanoparticles technology is employed the transport of the ECL ruthenium active species to the electrode surface does not occur by diffusion, the limitations due to the small diffusion coefficients of the large complexes are overcome.

Conclusions

Two homonuclear complexes **[Ru2−Lys]**$^{4+}$ and **[Ru3−LysLys]**$^{6+}$ have been synthesized. They contain two and three modified ruthenium tris(bipyridine) units linked by the amino acid lysine or the related dipeptide LysLys, respectively. Their redox and spectroscopic properties show that the ruthenium moieties remain independent and retain the electronic properties of the structurally closely related mononuclear compound **[Ru−Ref]**$^{2+}$. The ECL behavior was investigated in phosphate buffer solution (homogeneous assay) containing a nonionic surfactant and TPrA in excess. An increase of ECL intensity by 30% can be achieved for equimolar solutions of **[Ru2−Lys]**$^{4+}$ and **[Ru3−LysLys]**$^{6+}$ with respect to the reference mononuclear compound. The slow diffusion of the two multinuclear systems prevents stronger enhancement of the ECL signal. We have also demonstrated that the surfactant does not affect the spectroscopic properties of **[Ru2−Lys]**$^{4+}$ and **[Ru3−LysLys]**$^{6+}$, but it significantly increases the ECL output.

ECL experiments were then performed for larger dendritic complexes, **[Ru2−Dend]**$^{4+}$, **[Ru4−Dend]**$^{8+}$, and **[Ru8−Dend]**$^{16+}$, in both homogeneous assay and heterogeneous immunoassays. The results show that by means of the nanoparticle technology, the ECL signal of the immunoassays can increase linearly with the number of the active ruthenium centers. Large systems, however, such as **[Ru8−Dend]**$^{16+}$ may show intense background signal due to nonspecific binding, thus lowering the final ECL sensitivity. Further studies are currently in progress to reduce the ECL background.

Acknowledgment. M.S. thanks the European Commission for the financial support (Marie Curie Grant Contract No. ERBFMBICT983052). Part of the work at Roche was supported by the BMBF (Bundesministerium für Bildung und Forschung).

IC034435+